



Machining-Induced Damage and Corrosion Behavior of Monel-400 Alloy Under Cryogenic Cooling Conditions: A Sustainable Initiative

Ali Demirbaş¹ · Uğur Köklü^{2,3} · Sezer Morkavuk² · Khaled Giasin⁴ · Engin Kocaman⁵ · Murat Sarıkaya^{6,7} 

Received: 27 May 2024 / Revised: 19 August 2024 / Accepted: 5 September 2024
© The Author(s) 2024

Abstract

Monel-400 is a nickel-based heat-resistant superalloy (HRSA) that is primarily used in oil and marine applications. Machining Monel-400 alloy for marine applications usually involves drilling and milling operations for assembly purposes, which should meet the requirements to withstand use in salt-water environments (i.e. lower surface finish to reduce corrosion and lack of burrs for tight sealing between mating parts). However, drilling of Monel-400 alloy can be challenging due to its high strength and density, which induces thermal effects that can influence the surface and geometrical integrity of the holes. Consequently, the use of environmentally friendly cooling technologies, such as cryogenics, is an excellent alternative to mitigate these effects, something which has not been widely investigated in the open literature when drilling Monel-400 alloy. Therefore, the current study aims to investigate the machinability of Monel-400 alloy under dry and cryogenic cooling conditions. The effects of cutting parameters and the use of a cryogenic liquid nitrogen bath on the surface integrity and corrosion resistance of holes were evaluated. Additionally, cutting forces, chip formation, and corrosion performance were analyzed. The results showed that the cutting forces increased by up to 8% under cryogenic cooling. Under cryogenic conditions, reduced elastic deformation resulted in a smaller chip size. Both cutting conditions produced a smooth surface finish with a roughness value of less than 0.2 μm . Corrosion resistance was reduced under cryogenic conditions at spindle speed of 5000 rpm. The current work showcases that cryogenic cooling is recommended for drilling Monel-400 alloy used in marine applications, but care should be taken in employing optimal cutting parameters to mitigate any effects on corrosion resistance.

Keywords Sustainable manufacturing · Green drilling · Monel-400 alloy · Cryogenic cooling · Thrust force · Surface integrity · Corrosion

1 Introduction

The modern manufacturing industry handles the production of materials with properties that can meet the needs of various applications [1]. Nickel-based alloys are appealing to many industries due to properties such as high strength, resistance to high temperatures, and corrosion. These alloys are commonly used in the aerospace, defense, marine, and automotive industries, as well as in power generation, nuclear, pollution control, biomedical, and even musical instrument manufacturing [2–6]. Monel-400 alloy belongs to the nickel-copper alloy family, and has excellent corrosion resistance, high strength and toughness, and good properties at low temperatures [1, 7]. Owing to these properties, Monel-400 is widely used in many industries, especially in the automotive, marine, aerospace, nuclear, chemical, oil and gas refinery industries [1, 8, 9]. However, Monel-400 alloy has a high density of 8.8 g/cm³ and a high melting

✉ Murat Sarıkaya
msarikaya@sinop.edu.tr

¹ Natural and Applied Science, Karamanoglu Mehmetbey University, Karaman, Türkiye

² Department of Mechanical Engineering, Karamanoglu Mehmetbey University, Karaman, Türkiye

³ Department of Mechanical Engineering, Recep Tayyip Erdogan University, Rize, Türkiye

⁴ School of Mechanical and Design Engineering, University of Portsmouth, Portsmouth, UK

⁵ Department of Aerospace Engineering, Zonguldak Bulent Ecevit University, Zonguldak, Türkiye

⁶ Department of Mechanical Engineering, Sinop University, Sinop, Türkiye

⁷ Faculty of Mechanical Engineering, Opole University of Technology, 45-758 Opole, Poland

point of 1300–1350 °C [10], high heat resistance capacity, and high yield strength and toughness, making it a difficult-to-cut material by conventional machining processes [8, 9]. Various challenges arise during its machining such as highly induced cutting temperatures and cutting forces, rapid tool wear, and built-up edge (BUE) formation, as well as low surface quality [2, 8, 11]. To improve its machinability, various methods, such as hot-machining, photochemical machining, as well as cutting fluids have been employed [2]. Minimum quantity lubrication (MQL) utilizing eco-friendly nanofluids and cryogenic machining are commonly employed in green manufacturing to ensure effective lubrication and cooling, while simultaneously protecting the operator and preventing environmental contamination [12–15]. These environmentally friendly cooling and lubricating methods were applied by researchers during milling [16–24], turning [25–32], drilling [33–36] and grinding [37–45] operations of difficult-to-cut materials to improve their machinability.

Studies on the machinability of Monel-400 alloy have mainly focused on turning operations. In these studies, the effects of cutting parameters, workpiece temperatures, cutting tool coatings and nano-added cutting fluids on the process were investigated. It is reported that PVD-TiAlN coated tools showed good performance in terms of surface quality, nanoparticle-aided cutting fluid made significant contributions to tool wear behavior, and machinability improved as the workpiece temperature increased [1–5, 11]. Additionally, some researchers investigated plasma arc cutting and wire electrical discharge machining of Monel-400 [7–9, 46–48]. On the other hand, only a few studies are reported on the drilling of nickel-based superalloys, which found that they can be difficult to cut [49, 50], and these studies generally focused on Monel K500 rather than Monel 400. Jayakumar et al. [51] experimentally investigated the drilling of Monel K-500 using different cutting parameters, cutting tool material, and coolant considering material removal rate and surface quality and reported that tool material and feed rate have a significant effect on outputs. Sanjay et al. [52] optimized the cutting parameters in drilling Monel K500 alloy considering material removal rate, surface roughness, and tool wear using machine learning (ML) and artificial neural networks (ANN). Abdo et al. [53] investigated and

optimized the influence of the heat annealing process on the drilling machinability of Monel-400, considering cutting forces, surface roughness, and tool wear. In this study, the machinability behavior of the material heat treated at 700 and 1000 degrees was compared with the machinability behavior of the material at room temperature, and it was found that the thrust force and surface roughness decreased after heat treatment. When machining nickel-based alloys, due to low thermal conductivity, high strain hardening, and hot hardness, the heat generated during cutting cannot be removed sufficiently by the chip; thus, high temperatures occur in the cutting zone, which accelerates tool wear and poor surface quality, which leads to low machining efficiency [50, 54–59]. For this reason, it is of great importance to effectively dissipate the heat generated during the machining of difficult-to-cut materials such as nickel-based alloys [12]. Cryogenic machining, one of the most effective methods for cooling the cutting zone, workpiece, and cutting tool using environmentally friendly coolants during machining [12, 60], is preferred by researchers, especially for many difficult-to-cut materials such as Inconel-718 [34, 55, 61, 62], Nimonic alloys [63–66], Ti-6Al-4 V [67–70]. Although it is stated that cryogenic machining improves machinability in many materials, no study has been reported to date on the cryogenic machinability of Monel 400 alloy in drilling operations. Therefore, this work aims to fill this gap and investigate the machinability of Monel 400 alloy under a sustainable environment i.e., dry and cryogenic drilling conditions.

2 Materials and Methods

Monel-400 alloy with a thickness of 4 mm was used in the experiments. The chemical and mechanical properties of the Monel-400 alloy are given in Table 1.

The drilling experiments were conducted on a Quaser MV154C 3-axis vertical machining center under dry and cryogenic cutting conditions. The spindle speeds were set at 2500 and 5000 rpm, and the feed rates were varying between 100, 200, 300, 400, and 500 mm/min, as illustrated

Table 1 Chemical and mechanical properties of Monel-400 alloy

Chemical composition in mass %						
C	Cu	Fe	Mn	Ni	S	Si
Max 0.3	28–34	Max 2.5	Max 2	Min 63	Max 0.024	Max 0.5
Mechanical properties						
Tensile stress (MPa)		Yield strength (MPa)		Elongation (%)		Density (g/cc)
550		240		48		8.8

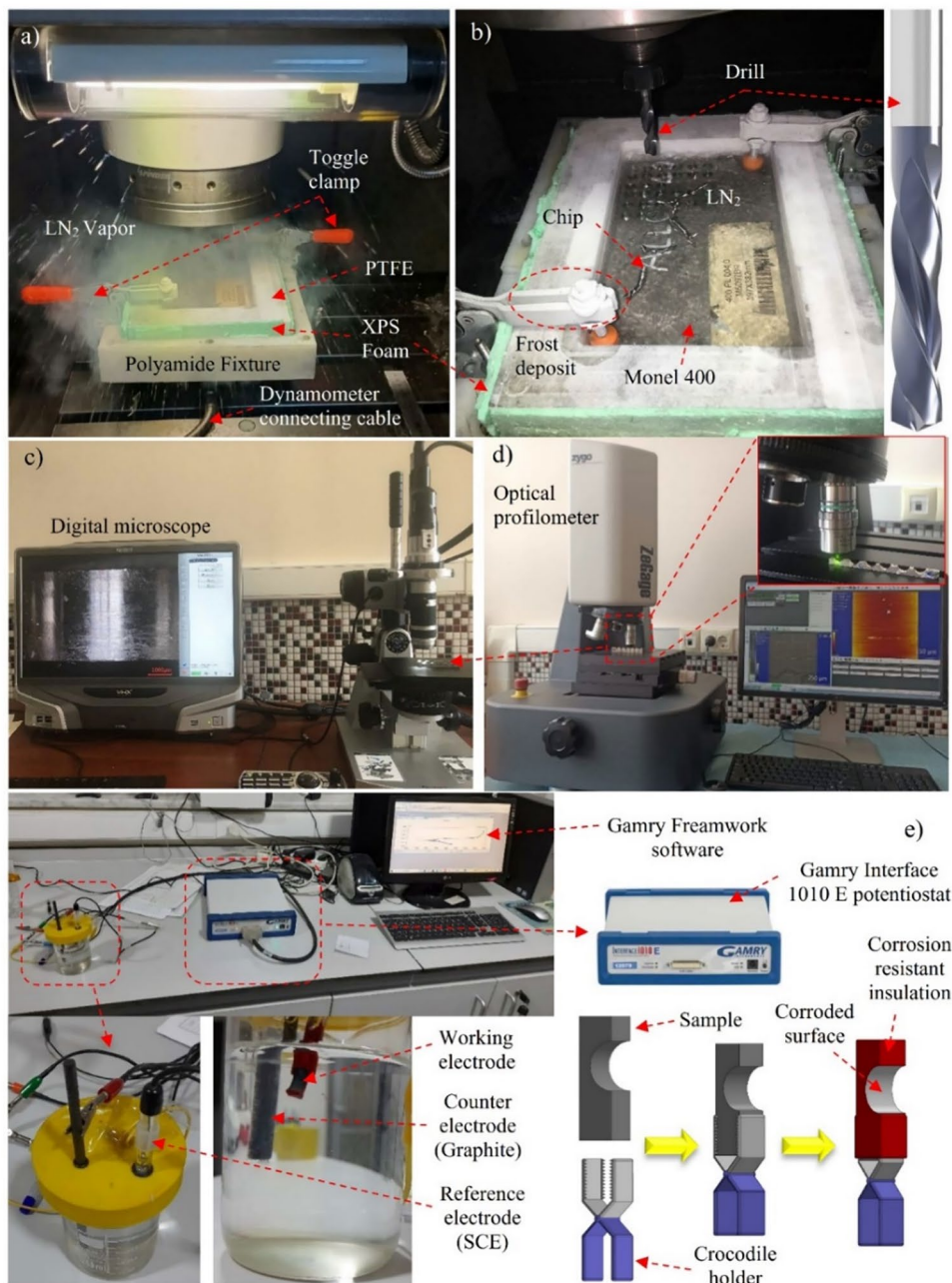
in Table 2. A total of 60 experiments were conducted, with each experiment consisting of three repetitions.

Table 2 Cutting parameters used in the experiments

Parameters	Level 1	Level 2	Level 3	Level 4	Level 5
Cooling environment	Dry	Cryogenic	-	-	-
Spindle speed (rpm)	2500	5000	-	-	-
Feed rate (mm/min)	100	200	300	400	500

The thrust force and torque during drilling were measured using KISTLER equipment (9257B force dynamometer, 5070 A amplifier, 5697 A data acquisition system) and DynoWare software. All drilling tests were carried out using a thermally insulated fixture that is placed on the top of the dynamometer, as shown in Fig. 1a. During cryogenic tests, the material was completely immersed in the liquid nitrogen ($-196\text{ }^{\circ}\text{C}$) bath. Solid carbide (WPC DIN 6537 series) helical drills with 8 mm diameter and 140° point angle were used as shown in Fig. 1b. The burrs at the hole exits, bore-hole surfaces and chips were inspected with Keyence VHX-900F digital microscope as presented in Fig. 1c. The

Fig. 1 Experimental set-up and measurement equipment



holes were further cut from their axes and the roughness and topography of the bore-hole surface were investigated with a Zygo Zegage optical profilometer (See Fig. 1d). Tests were also performed to investigate the effect of cutting parameters on the corrosion resistance of the machined surfaces using the Gamry 1010 E Potentiostat/Galvanostat as provided in Fig. 1e. In the corrosion tests, only the non-machined surfaces of the samples were isolated and working electrodes were prepared. All tests were carried out in 250 ml of 0.5 M NaCl solution. A potential range of -0.5 to $+1.5$ V and a scanning rate of 1 mV/sec were selected as test parameters. During the corrosion tests, a saturated calomel electrode was used as the reference electrode and a graphite electrode as a counter electrode. Tafel curves were obtained by potentiodynamic polarization method and Tafel parameters were extracted from the curves using Gamry-Echem computer software.

3 Results and Discussion

3.1 Cutting Forces Analysis

The effect of cutting parameters (spindle speed and feed rate) on thrust force and torque under dry and cryogenic conditions is given in Fig. 2a and b, respectively. According to Fig. 2a, increasing the spindle speed decreased cutting forces while increasing the feed rate increased cutting forces. At 2500 and 5000 rpm, the maximum thrust force generated at 500 mm/min feed rate and cryogenic conditions (1124 N and 642 N, respectively). The thrust force generated under cryogenic conditions is $\sim 8\%$ higher than those under dry cutting. Figure 2b shows that, in general,

the torque increased with increasing feed rate and decreased with increasing spindle speed. However, in cryogenic cutting conditions, severe fluctuations occurred, especially at low spindle speed (2500 rpm) were observed. The highest torque was measured at 500 mm/min feed rate under cryogenic conditions. The torque in all cryogenic cutting conditions was higher than that in dry cutting conditions. In previous studies, it was reported that, compared to dry machining, higher thrust force and torque are generated when drilling magnesium alloy [71], and fiber-reinforced plastics [72–74] using the cryogenic immersion approach, which is the cryogenic machining method used in this study. Some researchers [34, 36, 75] also noted that higher cutting forces occur when Inconel 718 is drilled under liquid nitrogen spraying method. Higher force generation in cryogenic machining can be explained in general terms by the fact that the hardness of the workpiece increases due to the extremely low boiling temperature of liquid nitrogen, resulting in greater resistance to plastic deformation [36, 75].

3.2 Chip Formation and Burr Analysis

Chip formation in the drilling process varies depending on many factors. These are workpiece material, cutting tool material, coating, geometry, point angle, use of coolant, cutting parameters, drilling strategies, etc. The chip morphology is one of the most common methods used to understand the deformation that occurs during metal cutting [76]. The chips were collected and examined with a digital microscope (Keyence VHX-900F) and SEM following the drilling experiments. Images of the chips under different cutting parameters are shown in Figs. 3 and 4 for dry and cryogenic conditions. It can be said that both cutting parameters and

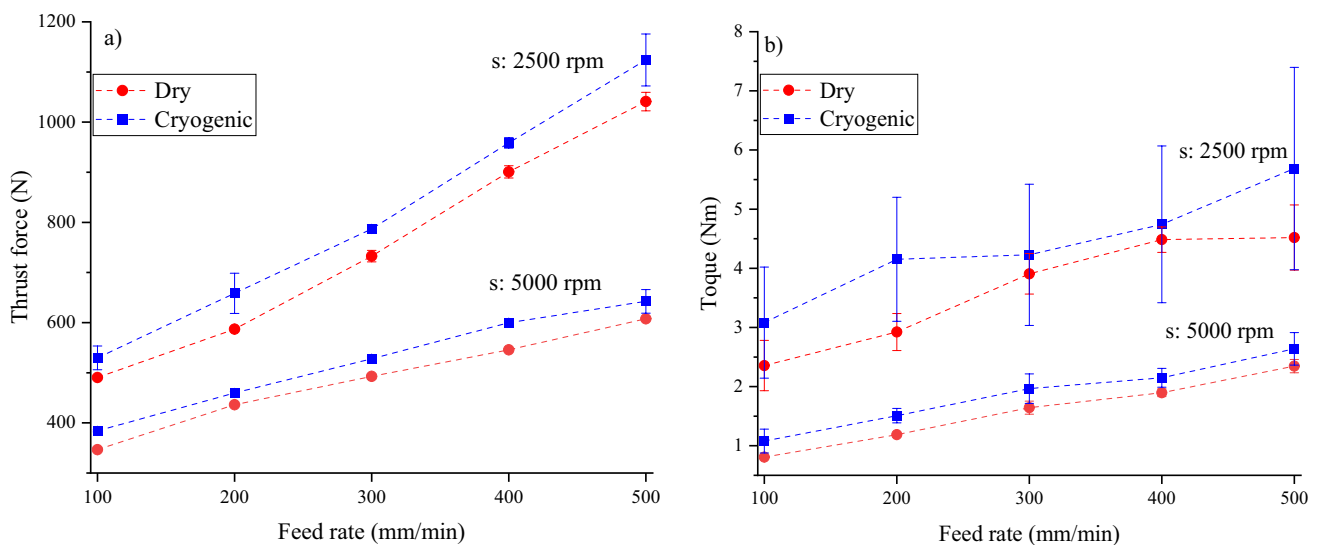


Fig. 2 The effect of the feed rate on **a** Thrust force **b** Torque under different spindle speeds and cooling conditions

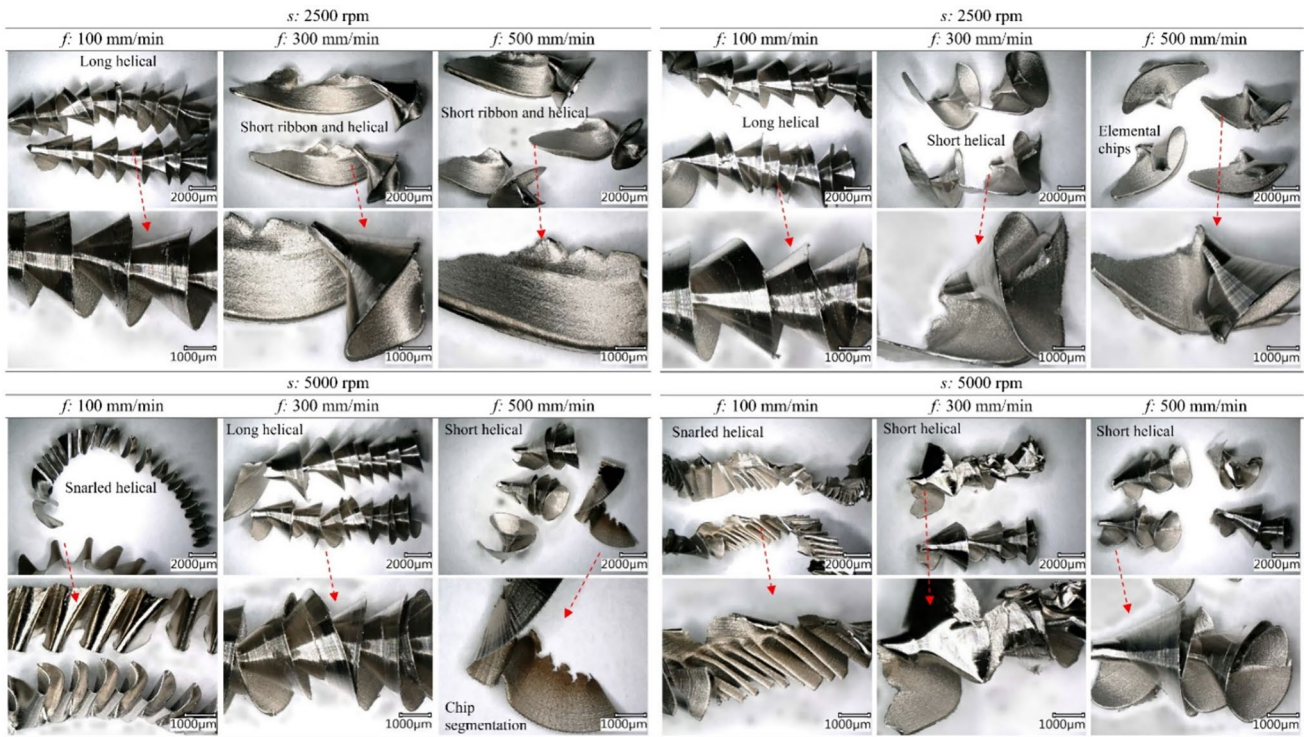


Fig. 3 Chip formation under dry and cryogenic cutting conditions (macroscopic view)

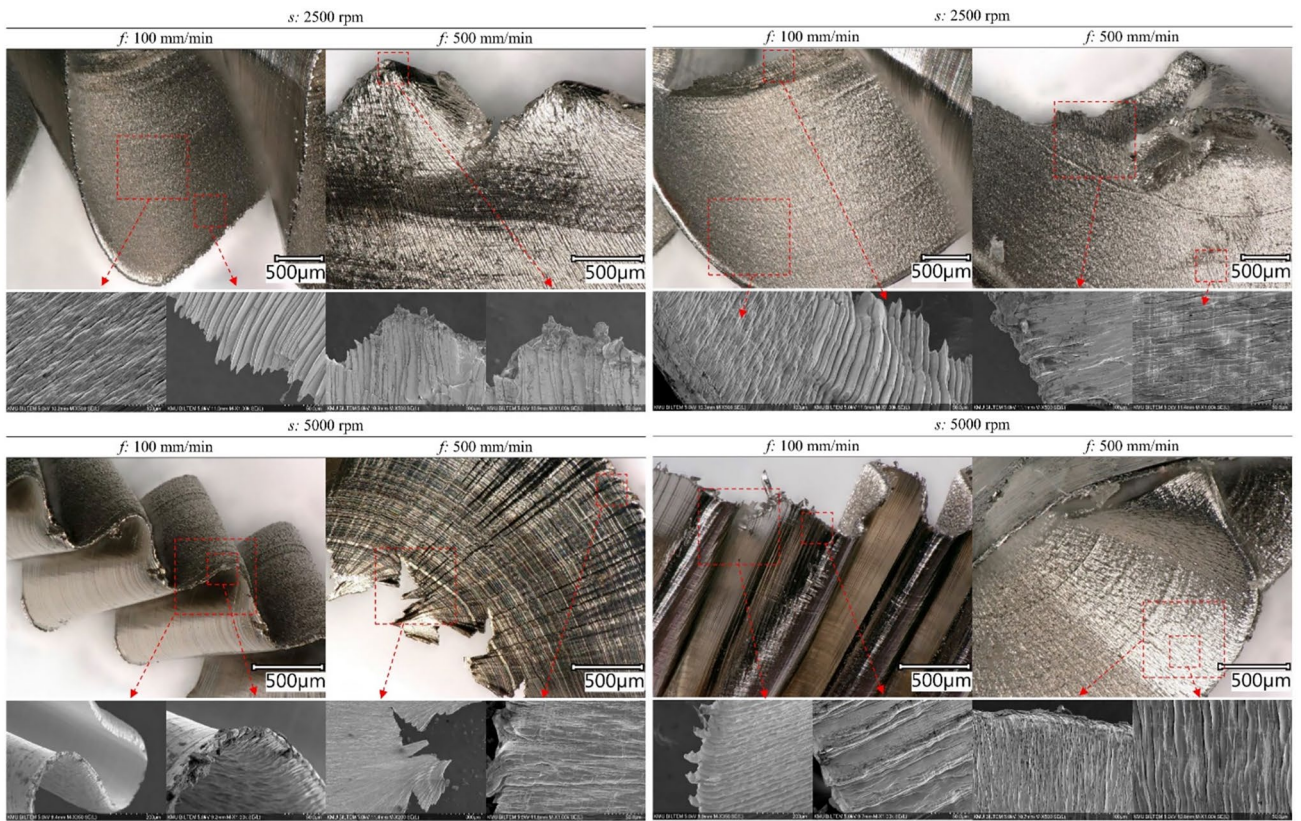


Fig. 4 Chip formation under dry and cryogenic cutting conditions (microscopic view)

cutting conditions (dry and cryogenic) had a direct effect on chip formation. Long helical chips were formed at low spindle speeds and low feed rates (300 mm/min) under dry conditions, as shown in Fig. 3, while the chip type changed from helical to ribbon as the feed rate increased. Snarled helical chips were formed at a low feed rate with increased deformation as spindle speed increased. As the feed rate increased, the chip type changed to long helical, and as the feed rate increased further, the chip type changed to short helical. In addition, under high spindle speed and feed rate, it was observed that chip segmentation occurs due to higher plastic deformation, depending on the effect of increasing temperature in the cutting zone. On the other hand, under cryogenic conditions, chips similar to those formed under dry conditions were formed by a combination of low spindle speed and feed rate. However, increasing the feed rate reduced chip size and formed elemental chips.

As previously highlighted in the literature, as the feed rate increases, the contact length between the chip and the tool increases, and this phenomenon affects the heat generation in the secondary deformation zone [17, 77]. For this reason, it can be said that the main effect of using cryogenic coolant becomes more evident at higher feed rates. When Figs. 3 and 4 are compared, the length of the chips obtained from cryogenic tests is shorter. The cryogenic temperatures of liquid nitrogen bath counteract the high cutting temperatures generated at the cutting zone, which limits elastic deformations and improves chip breakability.

During drilling, burrs may form on the hole edges at both the hole entrance and the hole exit, but the burrs at the hole exit are generally larger. Burrs affect dimensional accuracy, cause stress concentration and may also negatively affect fatigue and corrosion behavior. Burr size and shape may vary depending on the workpiece material, cutting parameters and therefore cutting forces and chip formation. Typically, there are three types of burr shapes: uniform, transient, and crown. A uniform burr usually starts with a fracture in the hole center due to the stress applied to the material by the tool and as the tool progressed, plastic deformation expands towards the hole edges and a uniform burr is formed with a second fracture. This type of burr is usually small in size and can be easily removed. In the second type of burr, transient, fracture occurs simultaneously at the hole center and edges. Therefore, the shape is between uniform and crown. Lastly, due to high plastic deformation, crown burrs are formed in large sizes and irregular geometry at the hole edges [78, 79].

The burrs formed at the hole exit were analyzed using a digital microscope, as shown in Fig. 5. In general, no severe burr formation was observed at the hole exits. However, slightly more burrs were formed in holes machined under dry-cutting conditions than under cryogenic conditions. It can also be seen that burr formation increased with increasing the feed rate. Finally, drilling at a lower spindle speed

(2500 rpm) resulted in higher burr formation compared to spindle speeds of 5000 rpm. Based on the information in the literature, it is seen that plastic deformation plays an important role in burr formation. It was also stated that uniform burr formation is observed at low cutting speeds and feed rates whereas crown burr formation is observed at high cutting speeds and feed rates and burr size increased depending on the feed rate when the spindle speed was high [78, 80]. Nevertheless, it is suggested that the material plastic deformation due to drilling exhibits an increasing brittle behavior, which consequently alters the formation of burrs.

3.3 Surface Roughness and Borehole Texture Analysis

The holes drilled under dry cutting were cross-sectioned from their center to examine the borehole surface quality using a digital microscope and optical profilometer (Fig. 6). The surface roughness of each hole was measured and reported, as shown in Fig. 7. The surface roughness (R_a) ranged between 0.1 and 0.2 μm which indicates a very smooth surface finish. The results show that cryogenic bath is more effective when drilling at higher spindle speeds, where higher temperatures are expected at the cutting zone. In general, the reduction in surface roughness (R_a) using cryogenic bath cooling ranged between 15–40% in comparison to dry conditions. However, at lower spindle speeds, the surface roughness fluctuated depending on the feed rate.

At 2500 rpm spindle speed and all feed rates under dry cutting conditions, macro-sized tool marks were observed on the borehole's surface. The marks on the surface were relatively reduced at 5000 rpm. Surface defects increased with increasing the feed rate. Tests performed at 2500 rpm spindle speed under dry cutting conditions show that it is not possible to use the surfaces without a second borehole finishing process. When all the experiments performed under dry conditions are evaluated, it can be said that the borehole surface formed in the experiment performed at 5000 rpm spindle speed and 100 mm/min feed rate is significantly better than the other holes. As a result, under dry-cutting conditions, a higher spindle speed and a lower feed rate improved the borehole surface quality. The cross-sectional view of the inner surfaces of the holes drilled under cryogenic conditions is given in Fig. 8. The use of cryogenic cooling helped eliminate the tool marks on the inner surface of the hole, which were observed during dry-cutting. Under cryogenic cutting conditions, the surface finish of all holes was generally the same. The surfaces of the boreholes sustained macroscale damage. Similar to what was observed under dry cutting conditions, increasing the spindle speed and decreasing the feed rate under cryogenic conditions also resulted in relatively smoother and cleaner surfaces. Some chip debris adhered to the hole surfaces under cryogenic

Fig. 5 Hole exit images



conditions due to difficulty in chip evacuation as the holes were fully submerged in liquid nitrogen. Such debris could be responsible for the fluctuations in the surface roughness readings. Although it affected the roughness values, less plastic deformation and tool mark formation under cryogenic conditions provided better surface quality.

3.4 Corrosion Analysis

In Fig. 9, the Tafel curves obtained as a result of the potentiodynamic polarization tests performed on the machined surfaces after drilling are given. It is understood that drilling

performed under dry conditions causes minor changes in the Tafel curves of Monel 400 alloy. By extrapolating Tafel curves, corrosion potential and corrosion current density can be obtained. Corrosion potential can be defined as the ability of the metal surface to lose electrons in an electrolyte liquid [81]. Also, corrosion potential is a measure of the tendency of the surface to corrosion. According to the Tafel parameters given in Table 3, no linear change was observed in the corrosion potentials by increasing the feed rate from 100 mm/min to 500 mm/min in the tests carried out at 2500 rpm under dry conditions. However, it is observed that there is a shift in the corrosion potentials to the positive side

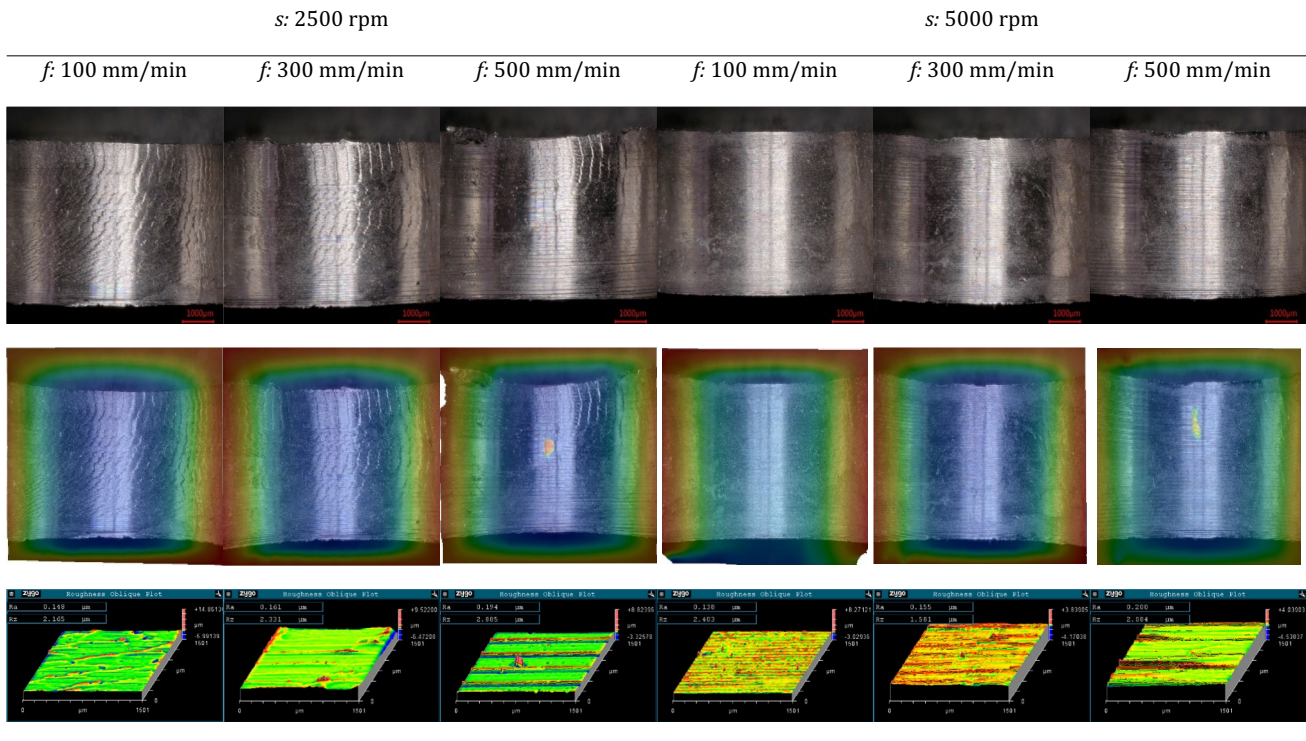


Fig. 6 Borehole imaging of tests performed under dry conditions

with increasing feed rate. On the other hand, the corrosion current density, which is an important parameter used in the evaluation of the electrochemical behavior of material [82, 83], decreases with increasing feed rate; that is, the corrosion resistance increases. In the corrosion tests carried out under dry conditions, at the same feed rates and by increasing the spindle speed to 5000 rpm, no linear change was also observed in the corrosion potential values. Current density values first decreased and then showed a slight increase at the 5000-rpm. In general, corrosion resistance increased with increasing spindle speed for the same feed rates in dry conditions.

In Fig. 9b, it is seen that drilling under cryogenic conditions causes more changes in Tafel curves than experiments performed under dry conditions. According to the Tafel test parameters given in Table 3, the corrosion potential value did not show a linear change with the increasing feed rate in the tests performed at 2500 rpm spindle speed, but the current density increased. In other words, corrosion resistance decreased with increasing feed rate. By increasing the feed rate from 100 mm/min to 500 mm/min, the corrosion current density value increased, that is, the corrosion resistance decreased. However, in the corrosion test of the sample drilled at 300 mm/min feed rate under cryogenic conditions, it was the material with the highest corrosion resistance among the samples drilled at 5000 rpm. In the tests carried out by increasing the spindle speed to 5000 rpm, the feed

rate did not cause a linear change in either the corrosion potential or the corrosion current density, depending on the change of machining parameters.

Within the scope of experimental studies, it was determined that changing drilling parameters had an effect on corrosion after drilling under both dry and cryogenic conditions. However, no significant relationship was found between the corrosion test results and drilling parameters. Overall, it can be stated that drilling at high speeds and in dry conditions increases the corrosion resistance of the machined surface. A similar result was previously reported by Reddy et al. [84] who found that the feed rate increased the surface roughness which in return increased corrosion.

In general, the corrosion test results are directly related to the surface condition and are expected to be correlated with the roughness values measured on the surfaces after drilling. However, in this study, no correlation was found between the roughness values measured on the surfaces after drilling and corrosion. Corrosion is closely related to some microstructural factors such as phases in the microstructure, distribution, friction and grain size of phases [85–87]. Also, the corrosion is directly related to the surface of the material, the surface topography has great importance in the relationship of drilling parameters with corrosion. As can be seen in Fig. 10, it is understood that the surface roughness in the surface topography of the hole is not similar throughout the entire surface and the roughness values increase

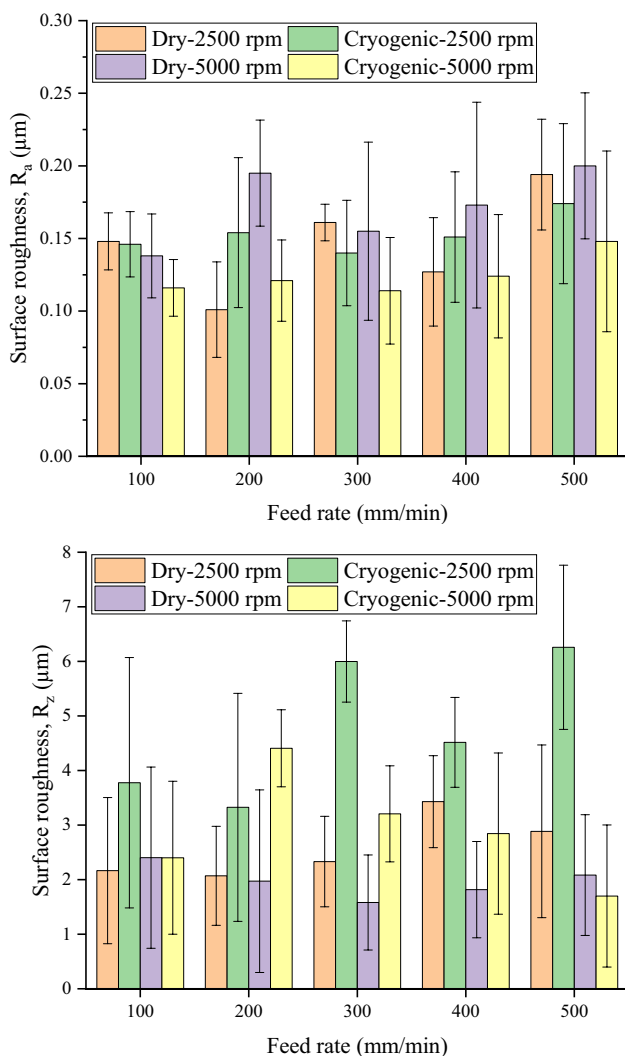


Fig. 7 Surface roughness (R_a and R_z) under dry and cryogenic conditions

and decrease locally. This situation increases the possibility of some areas dissolving faster and more preferentially than others in terms of corrosion. It is also understood from the surface images that craters are formed in some regions due to the drilling process on the surface. Such regions can induce pitting and cause various fluctuations in Tafel curves. In addition, Ni-Cu alloys are alloys with a tendency to passivation, as can be seen from the Tafel curves. During corrosion, traces of Ni and Cu elements containing chlorine and oxide are expected to form on the surface. This is seen in the EDS mapping (Fig. 10a), SEM (Fig. 10b), and EDS images of the sample which was drilled at 100 mm/min and 2500 rpm parameters under dry conditions.

It is known that this passivation after corrosion slows down the corrosion rate [88]. According to the SEM images taken after the corrosion test and shown in Fig. 11, it can be seen that there is an accumulation of corrosion products,

such as oxides and chlorides of Cu, Ni and Al elements, on the surfaces [89]. However, in some areas, it is observed that the passive layer on the surface is peeled off and crack formation occurs at the bottom. Pitting formation is also observed in some regions. It indicates that corrosion may have been accelerated as a result of the different surface finishes that occurred after the drilling process in the surface topography. Also, this may cause fluctuations in corrosion test parameters.

4 Conclusions

The current study investigates the drilling performance of Monel 400 alloy under dry and cryogenic cooling conditions. The aim is to evaluate the effect of cutting parameters (spindle speed and feed rate) and the use of a cryogenic bath cooling environment on the resulting cutting forces (thrust force and torque), chip formation, burr formation at the hole exit, and surface integrity. In addition, corrosion tests were performed to further assess the surface integrity of the machined holes. From the experimental results, the following can be concluded:

- The thrust force under cryogenic conditions was up to 8% higher than that under dry conditions due to increased resistance against plastic deformation during the drilling process.
- The chip size under cryogenic conditions was relatively smaller than that produced under dry conditions due to the increased brittleness of the workpiece, which in turn improved chip breakability during the drilling process.
- The surface roughness of machined holes did not exceed $0.2 \mu\text{m}$ and was reduced up to 40% under cryogenic conditions. However, at lower spindle speed, the surface quality under dry conditions was relatively better and free from feed and chip micro-damage marks.
- The cutting parameters do not have a linear effect on corrosion. Only in the drilling tests performed at 2500 rpm under dry conditions, did the corrosion current density decrease with increasing feed rate. Also, the corrosion resistance increased with increasing spindle speed for the same feed rates in dry conditions. The lowest corrosion rate was obtained at a feed rate of 300 mm/min and a spindle speed of 5000 rpm under dry conditions.
- Corrosion current density decreased with increasing feed rate in tests performed at 2500 rpm in cryogenic conditions. However, no linear change was observed depending on the feed rate in the tests performed at 5000 rpm in cryogenic conditions. Also, under cryogenic conditions, increasing the spindle speed from 2500 to 5000 rpm negatively affected the corrosion resistance.

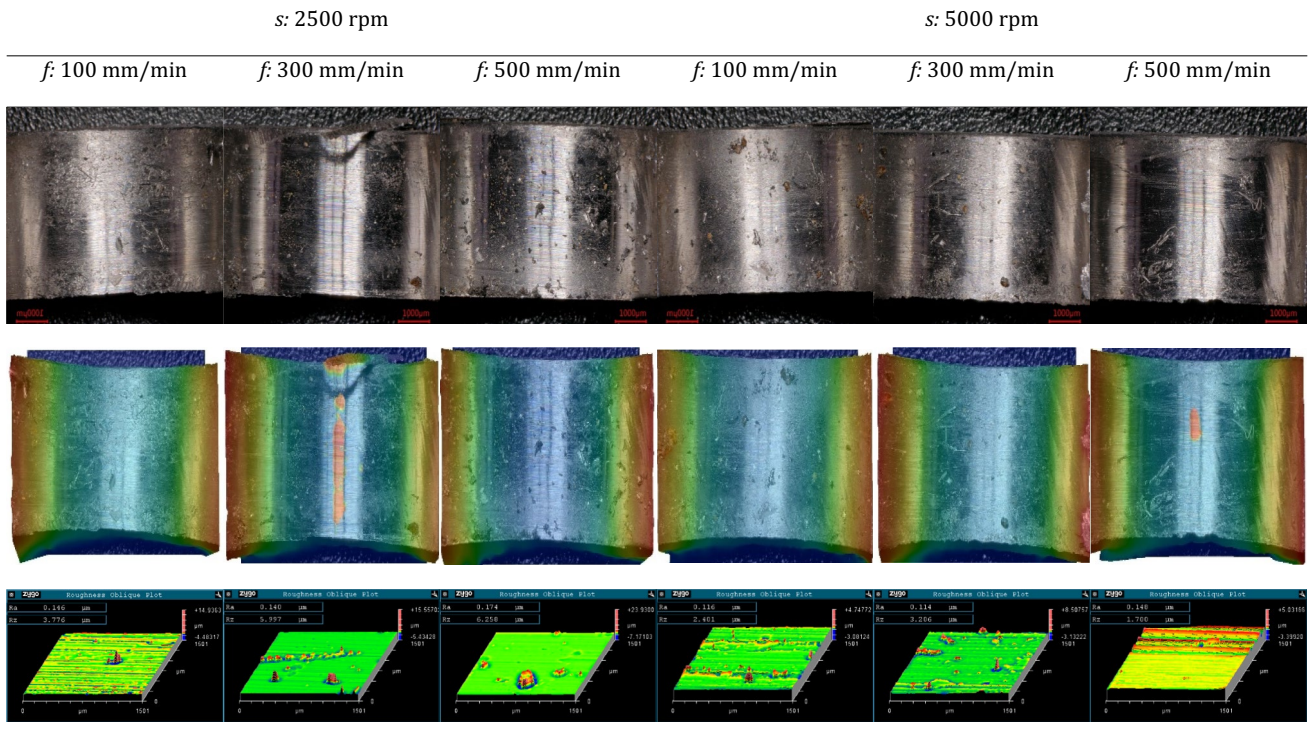


Fig. 8 Borehole condition under cryogenic conditions

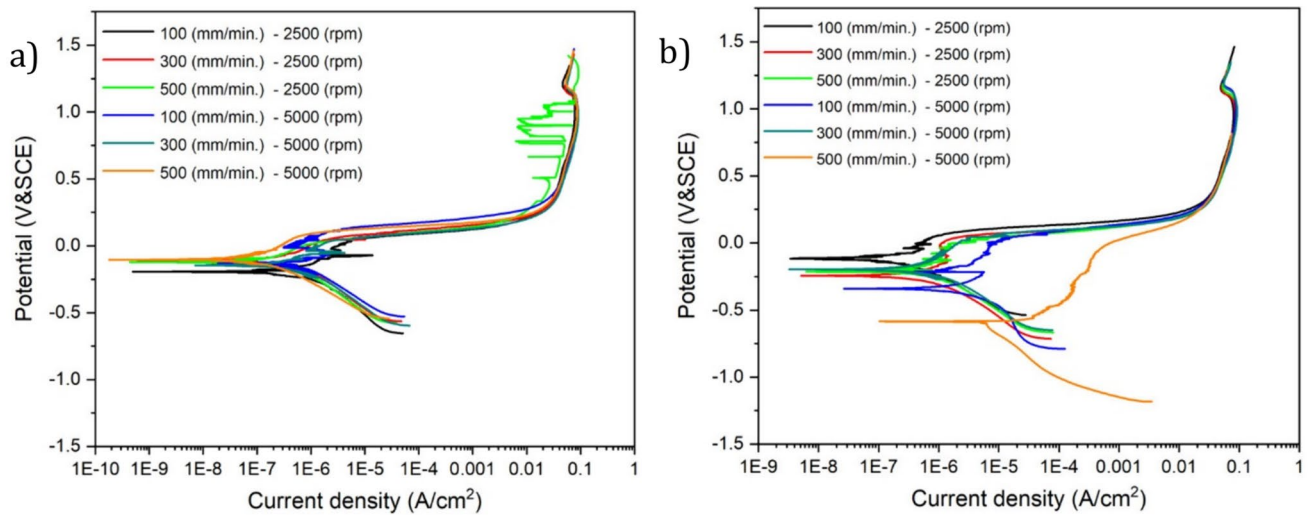


Fig. 9 Tafel curves a dry and b cryogenic drilling

- Despite an increase in thrust force under cryogenic conditions, positive effects were observed with regard to other machinability characteristics, including improve-

ments in hole quality and chip formation. Furthermore, future studies could investigate the drilling machinability of Monel 400 using MQL and conventional cool-

Table 3 Corrosion test parameters (dry and cryogenic drilling)

Sample	Dry		Cryogenic	
	E_{cor} (mV)	I_{cor} ($\mu\text{A}/\text{cm}^2$)	E_{cor} (mV)	I_{cor} ($\mu\text{A}/\text{cm}^2$)
2500 rpm, 100 mm/min	-194.318	0.487	-115.69	0.16
2500 rpm, 300 mm/min	-110.651	0.259	-244.4	0.324
2500 rpm, 500 mm/min	-121.323	0.146	-210.651	0.395
5000 rpm, 100 mm/min	-133.776	0.187	-339.683	2.35
5000 rpm, 300 mm/min	-143.567	0.086	-194.07	0.51
5000 rpm, 500 mm/min	-104.689	0.088	-596.452	5

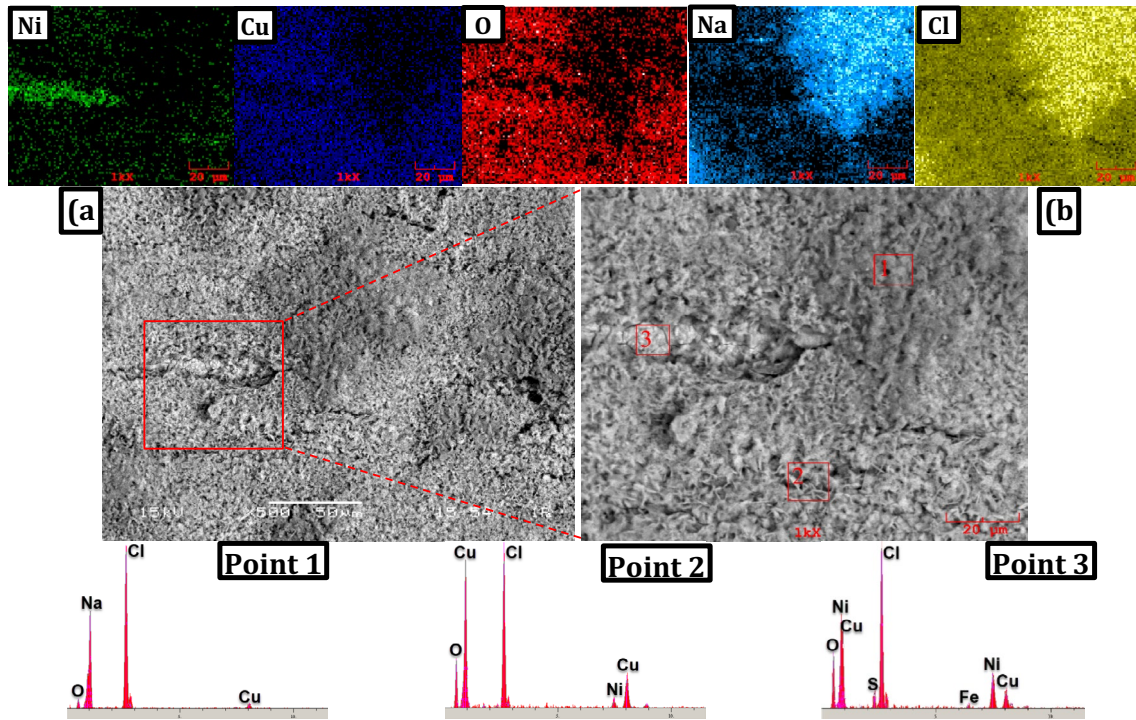
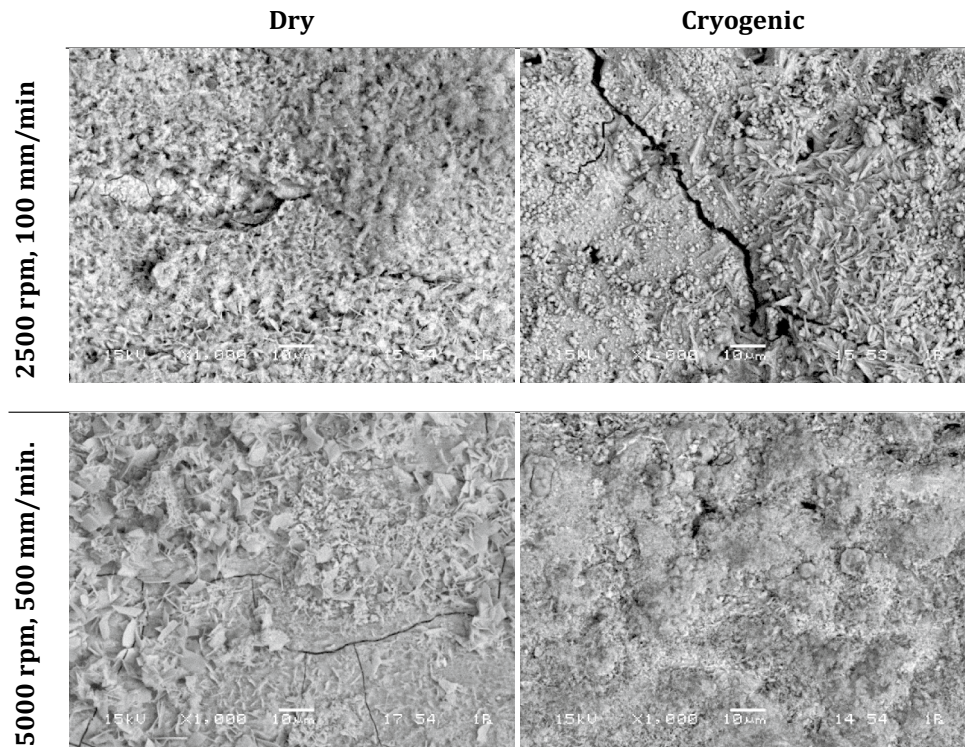


Fig. 10 Corroded surface of 100 mm/min—2500 rpm (dry drilling)

Fig. 11 SEM images of corroded surfaces



ing methods, as well as alternative coolants, and their impact on tool life.

Acknowledgements This work was supported by the Commission of Scientific Research Projects of Karamanoglu Mehmetbey University, Karaman-Turkey (Project No. 25-YL-21).

Funding This article is funded by Karamanoğlu Mehmetbey Üniversitesi, 25-YL-21, Uğur Köklü.

Data Availability Data included in article/supp. material/referenced in the article.

Declarations

Conflict of interest The authors declare no conflict of interest.

Open Access This article is licensed under a Creative Commons Attribution 4.0 International License, which permits use, sharing, adaptation, distribution and reproduction in any medium or format, as long as you give appropriate credit to the original author(s) and the source, provide a link to the Creative Commons licence, and indicate if changes were made. The images or other third party material in this article are included in the article's Creative Commons licence, unless indicated otherwise in a credit line to the material. If material is not included in the article's Creative Commons licence and your intended use is not permitted by statutory regulation or exceeds the permitted use, you will need to obtain permission directly from the copyright holder. To view a copy of this licence, visit <http://creativecommons.org/licenses/by/4.0/>.

References

1. Tayal, A., Kalsi, N. S., Gupta, M. K., Garcia-Collado, A., & Sarikaya, M. (2021). Reliability and economic analysis in sustainable machining of Monel 400 alloy. *Proceedings of the Institution of Mechanical Engineers, Part C: Journal of Mechanical Engineering Science*, 235(21), 5450–5466. <https://doi.org/10.1177/0954406220986818>
2. Kumar Parida, A., & Maity, K. (2019). Modeling of machining parameters affecting flank wear and surface roughness in hot turning of Monel-400 using response surface methodology (RSM). *Measurement*, 137, 375–381. <https://doi.org/10.1016/j.measurement.2019.01.070>
3. Parida, A. K., & Maity, K. (2018). Experimental investigation on tool life and chip morphology in hot machining of Monel-400. *Engineering Science and Technology, an International Journal*, 21(3), 371–379. <https://doi.org/10.1016/j.jestch.2018.04.003>
4. Dhananchezian, M. (2021). Experimental investigation on dry turned Monel 400 alloy surface parameters with uncoated and coated tool. *Materials Today: Proceedings*, 46, 8303–8306. <https://doi.org/10.1016/j.matpr.2021.03.264>
5. Parida, A. K., & Maity, K. (2018). Comparison the machinability of Inconel 718, Inconel 625 and Monel 400 in hot turning operation. *Engineering Science and Technology, an International Journal*, 21(3), 364–370. <https://doi.org/10.1016/j.jestch.2018.03.018>
6. Khadtare, A. N., Pawade, R., & Joshi, S. S. (2024). Experimental study in micro-drilling mechanism on heterogeneous structure of thermal barrier coated Inconel 718 superalloy. *International Journal of Precision Engineering and Manufacturing*, 25(3), 509–525. <https://doi.org/10.1007/s12541-023-00909-1>
7. Selvakumar, G., Sarkar, S., & Mitra, S. (2012). Experimental investigation on die corner accuracy for wire electrical discharge machining of Monel 400 alloy. *Proceedings of the*

- Institution of Mechanical Engineers, Part B: Journal of Engineering Manufacture*, 226(10), 1694–1704. <https://doi.org/10.1177/0954405412456660>
8. Rajamani, D., Ananthakumar, K., Balasubramanian, E., & Paulo, D. J. (2018). Experimental investigation and optimization of PAC parameters on Monel 400™ superalloy. *Materials and Manufacturing Processes*, 33(16), 1864–1873. <https://doi.org/10.1080/10426914.2018.1532085>
 9. Ananthakumar, K., Rajamani, D., Balasubramanian, E., & Paulo, D. J. (2019). Measurement and optimization of multi-response characteristics in plasma arc cutting of Monel 400™ using RSM and TOPSIS. *Measurement*, 135, 725–737. <https://doi.org/10.1016/j.measurement.2018.12.010>
 10. Küçük, Y., Döleker, K. M., Gök, M. S., Dal, S., Altınay, Y., & Erdoğan, A. (2022). Microstructure, hardness and high temperature wear characteristics of boronized Monel 400. *Surface and Coatings Technology*, 436, 128277. <https://doi.org/10.1016/j.surfcoat.2022.128277>
 11. Ross, N. S., Ganesh, M., Ananth, M. B. J., Kumar, M., Rai, R., Gupta, M. K., et al. (2023). Development and potential use of MWCNT suspended in vegetable oil as a cutting fluid in machining of Monel 400. *Journal of Molecular Liquids*, 382, 121853. <https://doi.org/10.1016/j.molliq.2023.121853>
 12. Khanna, N., Agrawal, C., Pimenov, D. Y., Singla, A. K., Machado, A. R., da Silva, L. R. R., et al. (2021). Review on design and development of cryogenic machining setups for heat resistant alloys and composites. *Journal of Manufacturing Processes*, 68, 398–422. <https://doi.org/10.1016/j.jmapro.2021.05.053>
 13. Pervaiz, S., Anwar, S., Qureshi, I., & Ahmed, N. (2019). Recent advances in the machining of titanium alloys using minimum quantity lubrication (MQL) based techniques. *International Journal of Precision Engineering and Manufacturing-Green Technology*, 6(1), 133–145. <https://doi.org/10.1007/s40684-019-00033-4>
 14. Singh, G., Aggarwal, V., & Singh, S. (2020). Critical review on ecological, economical and technological aspects of minimum quantity lubrication towards sustainable machining. *Journal of Cleaner Production*, 271, 122185. <https://doi.org/10.1016/j.jclepro.2020.122185>
 15. Yildiz, Y., & Nalbant, M. (2008). A review of cryogenic cooling in machining processes. *International Journal of Machine Tools and Manufacture*, 48(9), 947–964. <https://doi.org/10.1016/j.ijmactools.2008.01.008>
 16. Abdul Halim, N. H., Che Haron, C. H., & Abdul, G. J. (2020). Sustainable machining of hardened Inconel 718: A comparative study. *International Journal of Precision Engineering and Manufacturing*, 21(7), 1375–1387. <https://doi.org/10.1007/s12541-020-00332-w>
 17. Aramcharoen, A., & Chuan, S. K. (2014). An experimental investigation on cryogenic milling of Inconel 718 and its sustainability assessment. *Procedia CIRP*, 14, 529–534. <https://doi.org/10.1016/j.procir.2014.03.076>
 18. Duc, T. M., Long, T. T., & Tuan, N. M. (2021). Performance investigation of MQL parameters using nano cutting fluids in hard milling. *Fluids*, 6(7), 248.
 19. Haq, M. A. U., Hussain, S., Ali, M. A., Farooq, M. U., Mufti, N. A., Pruncu, C. I., et al. (2021). Evaluating the effects of nano-fluids based MQL milling of IN718 associated to sustainable productions. *Journal of Cleaner Production*, 310, 127463. <https://doi.org/10.1016/j.jclepro.2021.127463>
 20. Jain, A., Kumar, S., Bajpai, V., & Park, H. W. (2019). Replacement of hazard lubricants by green coolant in machining of Ti6Al4V: A 3D FEM approach. *International Journal of Precision Engineering and Manufacturing*, 20(6), 1027–1035. <https://doi.org/10.1007/s12541-019-00111-2>
 21. Park, K.-H., Suhaimi, M. A., Yang, G.-D., Lee, D.-Y., Lee, S.-W., & Kwon, P. (2017). Milling of titanium alloy with cryogenic cooling and minimum quantity lubrication (MQL). *International Journal of Precision Engineering and Manufacturing*, 18(1), 5–14. <https://doi.org/10.1007/s12541-017-0001-z>
 22. Pereira, O., Celaya, A., Urbikain, G., Rodríguez, A., Fernández-Valdivielso, A., & Lacalle, L. N. L. D. (2020). CO2 cryogenic milling of Inconel 718: Cutting forces and tool wear. *Journal of Materials Research and Technology*, 9(4), 8459–8468. <https://doi.org/10.1016/j.jmrt.2020.05.118>
 23. Şap, E., Usca, Ü. A., & Şap, S. (2024). Impacts of environmentally friendly milling of Inconel-800 superalloy on machinability parameters and energy consumption. *International Journal of Precision Engineering and Manufacturing-Green Technology*, 11(3), 781–797. <https://doi.org/10.1007/s40684-023-00579-4>
 24. Gao, Z., Zhang, H., Ji, M., Zuo, C., & Zhang, J. (2024). Influence of various cooling and lubrication conditions on tool wear and machining quality in milling Inconel 718. *International Journal of Precision Engineering and Manufacturing-Green Technology*, 11(2), 391–406. <https://doi.org/10.1007/s40684-023-00558-9>
 25. Bonfá, M. M., Costa, É. S., Sales, W. F., Amorim, F. L., Maia, L. H. A., & Machado, Á. R. (2019). Evaluation of tool life and workpiece surface roughness in turning of AISI D6 hardened steel using PCBN tools and minimum quantity of lubricant (MQL) applied at different directions. *The International Journal of Advanced Manufacturing Technology*, 103(1), 971–984. <https://doi.org/10.1007/s00170-019-03619-z>
 26. Dhananchezian, M., & Pradeep, K. M. (2011). Cryogenic turning of the Ti–6Al–4V alloy with modified cutting tool inserts. *Cryogenics*, 51(1), 34–40. <https://doi.org/10.1016/j.cryogenics.2010.10.011>
 27. Gan, Y., Wang, Y., Liu, K., Wang, S., Yu, Q., Che, C., et al. (2021). The development and experimental research of a cryogenic internal cooling turning tool. *Journal of Cleaner Production*, 319, 128787. <https://doi.org/10.1016/j.jclepro.2021.128787>
 28. Hadad, M., & Sadeghi, B. (2013). Minimum quantity lubrication-MQL turning of AISI 4140 steel alloy. *Journal of Cleaner Production*, 54, 332–343. <https://doi.org/10.1016/j.jclepro.2013.05.011>
 29. Ji, X., Li, B., Zhang, X., & Liang, S. Y. (2014). The effects of minimum quantity lubrication (MQL) on machining force, temperature, and residual stress. *International Journal of Precision Engineering and Manufacturing*, 15(11), 2443–2451. <https://doi.org/10.1007/s12541-014-0612-6>
 30. Kamata, Y., & Obikawa, T. (2007). High speed MQL finish-turning of Inconel 718 with different coated tools. *Journal of Materials Processing Technology*, 192–193, 281–286. <https://doi.org/10.1016/j.jmatprotec.2007.04.052>
 31. Singh, T., Dureja, J. S., Dogra, M., & Bhatti, M. S. (2018). Environment friendly machining of Inconel 625 under nano-fluid minimum quantity lubrication (NMQL). *International Journal of Precision Engineering and Manufacturing*, 19(11), 1689–1697. <https://doi.org/10.1007/s12541-018-0196-7>
 32. Yıldırım, Ç. V. (2020). Investigation of hard turning performance of eco-friendly cooling strategies: Cryogenic cooling and nano-fluid based MQL. *Tribology International*, 144, 106127. <https://doi.org/10.1016/j.triboint.2019.106127>
 33. Ganesh, M., & Arunkumar, N. (2024). A sustainable approach in deep hole drilling of Ti6Al4V: Effect of cryogenic cooling on hole parameters and its evaluation. *Journal of Manufacturing Processes*, 121, 343–360. <https://doi.org/10.1016/j.jmapro.2024.05.048>
 34. Khanna, N., Agrawal, C., Gupta, M. K., & Song, Q. (2020). Tool wear and hole quality evaluation in cryogenic Drilling of Inconel 718 superalloy. *Tribology International*, 143, 106084. <https://doi.org/10.1016/j.triboint.2019.106084>

35. Rahim, E. A., & Sasahara, H. (2011). A study of the effect of palm oil as MQL lubricant on high speed drilling of titanium alloys. *Tribology International*, 44(3), 309–317. <https://doi.org/10.1016/j.triboint.2010.10.032>
36. Shah, P., Bhat, P., & Khanna, N. (2021). Life cycle assessment of drilling Inconel 718 using cryogenic cutting fluids while considering sustainability parameters. *Sustainable Energy Technologies and Assessments*, 43, 100950. <https://doi.org/10.1016/j.seta.2020.100950>
37. Abedrabbo, F., Madariaga, A., Soriano, D., Pérez, M., Butano, E., Fernández, R., et al. (2023). Influence of cryogenic grinding surface on fatigue performance of carburised 27MnCr5. *Journal of Materials Research and Technology*, 23, 1792–1804. <https://doi.org/10.1016/j.jmrt.2023.01.111>
38. Awale, A. S., Chaudhari, A., Kumar, A., Khan Yusufzai, M. Z., & Vashista, M. (2022). Synergistic impact of eco-friendly nano-lubricants on the grindability of AISI H13 tool steel: A study towards clean manufacturing. *Journal of Cleaner Production*, 364, 132686. <https://doi.org/10.1016/j.jclepro.2022.132686>
39. Awale, A. S., Srivastava, A., Vashista, M., & Khan Yusufzai, M. Z. (2019). Influence of minimum quantity lubrication on surface integrity of ground hardened H13 hot die steel. *The International Journal of Advanced Manufacturing Technology*, 100(1), 983–997. <https://doi.org/10.1007/s00170-018-2777-0>
40. Awale, A. S., Vashista, M., & Khan Yusufzai, M. Z. (2021). Application of eco-friendly lubricants in sustainable grinding of die steel. *Materials and Manufacturing Processes*, 36(6), 702–712. <https://doi.org/10.1080/10426914.2020.1866187>
41. Balan, A. S. S., Chidambaram, K., Kumar, A. V., Krishnaswamy, H., Pimenov, D. Y., Giasin, K., et al. (2021). Effect of cryogenic grinding on fatigue life of additively manufactured maraging steel. *Materials*, 14(5), 1245.
42. Lee, P.-H., Lee, S. W., Lim, S.-H., Lee, S.-H., Ko, H. S., & Shin, S.-W. (2015). A study on thermal characteristics of micro-scale grinding process using nanofluid minimum quantity lubrication (MQL). *International Journal of Precision Engineering and Manufacturing*, 16(9), 1899–1909. <https://doi.org/10.1007/s12541-015-0247-2>
43. Lopes, J. C., Ávila, B. N., de Souza, R. M., Garcia, M. V., Ribeiro, F. S. F., de Mello, H. J., et al. (2021). Grinding comparative analysis between different proportions of water-oil applied to MQL technique and industrial production cost towards a green manufacturing. *The International Journal of Advanced Manufacturing Technology*, 113(5), 1281–1293. <https://doi.org/10.1007/s00170-021-06625-2>
44. Manimaran, G., Pradeep Kumar, M., & Venkatasamy, R. (2014). Influence of cryogenic cooling on surface grinding of stainless steel 316. *Cryogenics*, 59, 76–83. <https://doi.org/10.1016/j.cryogenics.2013.11.005>
45. Sharma, A., Chaudhari, A., Diwakar, V., Awale, A. S., Yusufzai, M. Z. K., & Vashista, M. (2024). Implementation of hybrid CryoMQL sustainable lubri-cooling to enhance the grindability and surface integrity of tool steel. *Journal of Manufacturing Processes*, 119, 16–31. <https://doi.org/10.1016/j.jmapro.2024.03.040>
46. Kumar, N. E. A., & Babu, A. S. (2018). Influence of input parameters on the near-dry WEDM of Monel alloy. *Materials and Manufacturing Processes*, 33(1), 85–92. <https://doi.org/10.1080/10426914.2017.1279297>
47. Kumar, V., Kumar, V., & Jangra, K. K. (2015). An experimental analysis and optimization of machining rate and surface characteristics in WEDM of Monel-400 using RSM and desirability approach. *Journal of Industrial Engineering International*, 11(3), 297–307. <https://doi.org/10.1007/s40092-015-0103-0>
48. Manikandan, K., Ranjith Kumar, P., Raj Kumar, D., & Palanikumar, K. (2020). Machinability evaluation and comparison of Incoloy 825, Inconel 603 XL, Monel K400 and Inconel 600 super alloys in wire electrical discharge machining. *Journal of Materials Research and Technology*, 9(6), 12260–12272. <https://doi.org/10.1016/j.jmrt.2020.08.049>
49. Thellaputta, G. R., Chandra, P. S., & Rao, C. S. P. (2017). Machinability of nickel based superalloys: A review. *Materials Today: Proceedings*, 4(2), 3712–3721. <https://doi.org/10.1016/j.matpr.2017.02.266>
50. Wang, R., Yang, D., Wang, W., Wei, F., Lu, Y., & Li, Y. (2022). Tool wear in nickel-based superalloy machining: An overview. *Processes*, 10(11), 2380.
51. Jayakumar, K., Koundinya, K. A., Jayakumar, T., Harshal, M., & Gopinath, G. (2020). Experimental studies on the effect of drilling parameters on Monel Alloy. *Materials Science Forum: Trans Tech Publ*, 979, 137–141.
52. Sanjay, C., Alsamhan, A., & Abidi, M. H. (2022). Multi response optimization of machining parameters for an annealed Monel K 500 alloy in drilling using machine learning techniques and ANN. *Journal of Intelligent & Fuzzy Systems*, 42, 5605–5625. <https://doi.org/10.3233/JIFS-212087>
53. Abdo, B. M. A., Almuzaiqer, R., Noman, M. A., & Chintakindi, S. (2023). Investigation of heat annealing and parametric optimization for drilling of Monel-400 alloy. *Journal of Manufacturing and Materials Processing*, 7(5), 170.
54. Pervaiz, S., Rashid, A., Deiab, I., & Nicolescu, M. (2014). Influence of tool materials on machinability of titanium- and nickel-based alloys: A review. *Materials and Manufacturing Processes*, 29(3), 219–252. <https://doi.org/10.1080/10426914.2014.880460>
55. Pusavec, F., Hamdi, H., Kopac, J., & Jawahir, I. S. (2011). Surface integrity in cryogenic machining of nickel based alloy—Inconel 718. *Journal of Materials Processing Technology*, 211(4), 773–783. <https://doi.org/10.1016/j.jmatprotec.2010.12.013>
56. Thakur, A., & Gangopadhyay, S. (2016). State-of-the-art in surface integrity in machining of nickel-based super alloys. *International Journal of Machine Tools and Manufacture*, 100, 25–54. <https://doi.org/10.1016/j.ijmactools.2015.10.001>
57. Güven, S., Karataş, M. A., & Gökkaya, H. (2024). A Study on optimum machinability of NiTi shape memory alloy via AWJ. *International Journal of Precision Engineering and Manufacturing*, 25(3), 555–564. <https://doi.org/10.1007/s12541-023-00946-w>
58. Yoon, I.-C., Kang, I.-S., Park, K.-H., Heo, J.-Y., Lee, J.-R., & Jung, Y.-C. (2024). Three-dimensional measurement and finite-element simulation for tool wear estimation in cutting of inconel 718 superalloy. *International Journal of Precision Engineering and Manufacturing*, 25(1), 21–34. <https://doi.org/10.1007/s12541-023-00902-8>
59. Wang, Q., Chen, X., An, Q., Chen, M., Guo, H., & He, Y. (2024). Multi-objective optimization strategy for continuous drilling parameters of superalloys. *International Journal of Precision Engineering and Manufacturing-Green Technology*, 11(4), 1115–1132. <https://doi.org/10.1007/s40684-023-00591-8>
60. Kaynak, Y., Lu, T., & Jawahir, I. S. (2014). Cryogenic machining-induced surface integrity: A review and comparison with Dry, MQL, and flood-cooled machining. *Machining Science and Technology*, 18(2), 149–198. <https://doi.org/10.1080/10910344.2014.897836>
61. Kaynak, Y. (2014). Evaluation of machining performance in cryogenic machining of Inconel 718 and comparison with dry and MQL machining. *The International Journal of Advanced*

- Manufacturing Technology*, 72(5), 919–933. <https://doi.org/10.1007/s00170-014-5683-0>
62. Kenda, J., Pusavec, F., & Kopac, J. (2011). Analysis of residual stresses in sustainable cryogenic machining of nickel based alloy—inconel 718. *Journal of Manufacturing Science and Engineering*. <https://doi.org/10.1115/1.4004610>
 63. Chetan, N., Ghosh, S., & Rao, P. V. (2016). Environment friendly machining of Ni–Cr–Co based super alloy using different sustainable techniques. *Materials and Manufacturing Processes*, 31(7), 852–859. <https://doi.org/10.1080/10426914.2015.1037913>
 64. Jadhav, P. S., & Mohanty, C. P. (2022). Performance assessment of energy efficient and eco-friendly turning of Nimonic C-263: A comparative study on MQL and cryogenic machining. *Proceedings of the Institution of Mechanical Engineers, Part B: Journal of Engineering Manufacture.*, 236(8), 1125–1140. <https://doi.org/10.1177/09544054211061961>
 65. Nimel Sworna Ross, K., & Manimaran, G. (2019). Effect of cryogenic coolant on machinability of difficult-to-machine Ni–Cr alloy using PVD-TiAlN coated WC tool. *Journal of the Brazilian Society of Mechanical Sciences and Engineering*, 41(1), 44. <https://doi.org/10.1007/s40430-018-1552-3>
 66. Patel, T., Khanna, N., Yadav, S., Shah, P., Sarikaya, M., Singh, D., et al. (2021). Machinability analysis of nickel-based superalloy Nimonic 90: A comparison between wet and LCO₂ as a cryogenic coolant. *The International Journal of Advanced Manufacturing Technology*, 113(11), 3613–3628. <https://doi.org/10.1007/s00170-021-06793-1>
 67. Hong, S. Y., Markus, I., & Jeong, W.-C. (2001). New cooling approach and tool life improvement in cryogenic machining of titanium alloy Ti-6Al-4V. *International Journal of Machine Tools and Manufacture*, 41(15), 2245–2260. [https://doi.org/10.1016/S0890-6955\(01\)00041-4](https://doi.org/10.1016/S0890-6955(01)00041-4)
 68. Perçin, M., Aslantas, K., Uçun, İ., Kaynak, Y., & Çicek, A. (2016). Micro-drilling of Ti-6Al-4V alloy: The effects of cooling/lubricating. *Precision Engineering*, 45, 450–462. <https://doi.org/10.1016/j.precisioneng.2016.02.015>
 69. Shah, P., Khanna, N., Singla, A. K., & Bansal, A. (2021). Tool wear, hole quality, power consumption and chip morphology analysis for drilling Ti-6Al-4V using LN₂ and LCO₂. *Tribology International*, 163, 107190. <https://doi.org/10.1016/j.triboint.2021.107190>
 70. Shokrani, A., & Newman, S. T. (2019). A new cutting tool design for cryogenic machining of Ti-6Al-4V titanium alloy. *Materials*, 12(3), 477.
 71. Koklu, U., & Coban, H. (2020). Effect of dipped cryogenic approach on thrust force, temperature, tool wear and chip formation in drilling of AZ31 magnesium alloy. *Journal of Materials Research and Technology.*, 9(3), 2870–2880. <https://doi.org/10.1016/j.jmrt.2020.01.038>
 72. Giasin, K., Barouni, A., Dhakal, H. N., Featherson, C., Redouane, Z., Morkavuk, S., et al. (2021). Microstructural investigation and hole quality evaluation in S2/FM94 glass-fibre composites under dry and cryogenic conditions. *Journal of Reinforced Plastics and Composites.*, 40(7–8), 273–293. <https://doi.org/10.1177/0731684420958479>
 73. Koklu, U., & Morkavuk, S. (2019). Cryogenic drilling of carbon fiber-reinforced composite (CFRP). *Surface Review and Letters*, 26(09), 1950060. <https://doi.org/10.1142/s0218625x19500604>
 74. Basmaci, G., Yoruk, A. S., Koklu, U., & Morkavuk, S. (2017). Impact of cryogenic condition and drill diameter on drilling performance of CFRP. *Applied Sciences*, 7(7), 667.
 75. Uçak, N., & Çiçek, A. (2018). The effects of cutting conditions on cutting temperature and hole quality in drilling of Inconel 718 using solid carbide drills. *Journal of Manufacturing Processes.*, 31, 662–673. <https://doi.org/10.1016/j.jmapro.2018.01.003>
 76. Köklü, U., Koçar, O., Morkavuk, S., Giasin, K., & Ayer, Ö. (2022). Influence of extrusion parameters on drilling machinability of AZ31 magnesium alloy. *Proceedings of the Institution of Mechanical Engineers, Part E: Journal of Process Mechanical Engineering.*, 236(5), 2082–2094. <https://doi.org/10.1177/09544089221080820>
 77. Bermingham, M. J., Kirsch, J., Sun, S., Palanisamy, S., & Dargusch, M. S. (2011). New observations on tool life, cutting forces and chip morphology in cryogenic machining Ti-6Al-4V. *International Journal of Machine Tools and Manufacture.*, 51(6), 500–511. <https://doi.org/10.1016/j.ijmachtools.2011.02.009>
 78. Aamir, M., Giasin, K., Tolouei-Rad, M., & Vafadar, A. (2020). A review: Drilling performance and hole quality of aluminium alloys for aerospace applications. *Journal of Materials Research and Technology.*, 9(6), 12484–12500. <https://doi.org/10.1016/j.jmrt.2020.09.003>
 79. Yazman, Ş, Köklü, U., Urtekin, L., Morkavuk, S., & Gemi, L. (2020). Experimental study on the effects of cold chamber die casting parameters on high-speed drilling machinability of casted AZ91 alloy. *Journal of Manufacturing Processes.*, 57, 136–152. <https://doi.org/10.1016/j.jmapro.2020.05.050>
 80. Avila, M. C., Gardner, J. D., Reich-Weiser, C., Vijayaraghavan, A., & Dornfeld, D. (2006). Strategies for burr minimization and cleanability in aerospace and automotive manufacturing. *SAE Transactions Journal of Aerospace*, 114(1), 1073–1082.
 81. Zhang, X. G. (1996). Corrosion potential and corrosion current. *Corrosion and Electrochemistry of Zinc* (pp. 125–156). Boston: Springer.
 82. Frankel, G. S. (2016). Fundamentals of corrosion kinetics. In A. E. Hughes, J. M. C. Mol, M. L. Zheludkevich, & R. G. Buchheit (Eds.), *Active Protective Coatings: New-Generation Coatings for Metals* (pp. 17–32). Netherlands: Springer.
 83. Kocaman, E., Kılınc, B., Şen, Ş., & Şen, U. (2020). Krom içeriğinin Fe(18-x)Cr_xB₂ (X = 3, 4, 5) sert dolgu elektrotunda mikroyapı, aşınma ve korozyon davranışı üzerindeki etkisi. *Gazi Üniversitesi Mühendislik Mimarlık Fakültesi Dergisi*, 36(1), 177–190. <https://doi.org/10.17341/gazimmfd.689230>
 84. Reddy, U., Dubey, D., Panda, S. S., Ireddy, N., Jain, J., Mondal, K., et al. (2021). Effect of surface roughness induced by milling operation on the corrosion behavior of magnesium alloys. *Journal of Materials Engineering and Performance*, 30(10), 7354–7364. <https://doi.org/10.1007/s11665-021-05933-8>
 85. Jomy, J., Sharma, S., Prabhu, P. R., Hiremath, P., & Prabhu, D. (2023). Microstructural changes and their influence on corrosion post-annealing treatment of copper and AISI 5140 steel in 3.5 wt% NaCl medium. *Cogent Engineering*, 10(1), 2244770. <https://doi.org/10.1080/23311916.2023.2244770>
 86. Kocaman, E. (2023). Effect of Al5Ti1B and Al8B on the microstructure, wear and corrosion behavior of CuZn19Al6 bronze alloy. *Materials Today Communications*, 36, 106551. <https://doi.org/10.1016/j.mtcomm.2023.106551>
 87. Kocaman, E., Aydın, H., Yiğit, K., Çalışkan, F., & Savaş, Ö. (2024). Corrosion behaviour of Al/(TiB₂ + -Al₃Ti)-based functional grade metal matrix composite by sedimentation method. *Transactions of the Indian Institute of Metals*. <https://doi.org/10.1007/s12666-024-03301-3>
 88. Sherif, E.-S.M., Almajid, A. A., Bairamov, A. K., & Al-Zahrani, E. (2011). Corrosion of Monel-400 in aerated stagnant Arabian gulf seawater after different exposure intervals. *International*

Journal of Electrochemical Science, 6(11), 5430–5444. [https://doi.org/10.1016/S1452-3981\(23\)18418-5](https://doi.org/10.1016/S1452-3981(23)18418-5)

89. He, Z., Chen, B., Zhou, B., Liu, F., Hu, Q., Qin, Z., et al. (2023). Effect of TiC precipitation on the corrosion behavior of Monel K500 alloy in 3.5 wt% NaCl solution. *Corrosion Science*, 211, 110886. <https://doi.org/10.1016/j.corsci.2022.110886>

Publisher's Note Springer Nature remains neutral with regard to jurisdictional claims in published maps and institutional affiliations.



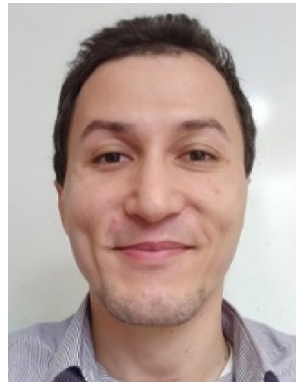
Ali Demirbaş received a MSC degree in Mechanical Engineering in 2023, from Karamanoğlu Mehmetbey University. His research interests include machine design and machinability. He is currently working on food machinery manufacturing industry as an engineer.



Uğur Köklü received a PhD degree in Mechanical Engineering in 2009 and became an Associate Professor in the same field in 2014. Since 2019, he has been working as a professor at the Karamanoğlu Mehmetbey University, Department of Mechanical engineering. His research interests are machinability of metals and composites and has contributed to the field through the publication of numerous articles on these topics.



Sezer Morkavuk received a BSc degree in Mechanical Engineering in 2013, and a PhD degree in the same field in 2023. His research interests include production and mechanical testing of polymer composites, as well as the machinability of engineering materials. He currently works as a research assistant at Karamanoğlu Mehmetbey University, Mechanical Engineering Department.



Khaled Giasin is a senior lecturer in the school of Mechanical and Design Engineering in the faculty of Technology at the university of Portsmouth. His main research background is on machining aerospace materials using experimental and numerical techniques. Before joining the University of Portsmouth, He worked at Cardiff University as a postdoctoral research associate project officer in ASTUTE2020 (A European funded project). He also authored over 100 publications in peer reviewed journals

and international conferences, he is the supervisor of several PhD projects and currently working with leading academic experts in close collaboration with academics and industry, developing impactful, state-of-the-art research-based solutions to the real-world problems facing advanced manufacturing.



Engin Kocaman is an Associate Professor in the Department of Aerospace Engineering, Zonguldak Bulent Ecevit University, Türkiye. He received the Ph.D. degree from Sakarya University in 2021. His current research interests are casting, hardfacing, solidification, wear and corrosion of ferrous and non-ferrous metals.



Murat Sarıkaya received his PhD from Gazi University, Turkey, in 2014. He became an Associate Professor in Mechanical Engineering in 2017, and since 2023, he has been a Full Professor at Department of Mechanical Engineering, Sinop University, Turkey. His main research areas include machining, sustainable manufacturing, and additive manufacturing, and he has published numerous articles in renowned scientific journals in these fields.